

AD-A168 125

GAIN ANISOTROPY IN LOW PRESSURE CHEMICAL LASERS(U)
AEROSPACE CORP EL SEGUNDO CA AEROPHYSICS LAB H NIRELS
15 APR 86 TR-0086(6060)-4 SD-TR-86-21 F04701-85-C-0086

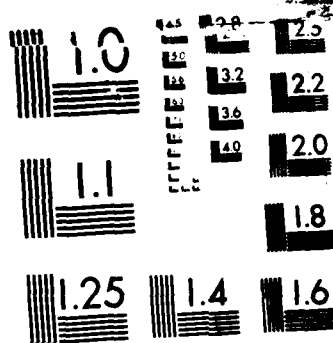
1/1

UNCLASSIFIED

F/G 20/5

NL





MICROCOPY RESOLUTION TEST CHART
NATIONAL BUREAU OF STANDARDS-1963-A

12

AD-A168 125

Gain Anisotropy in Low Pressure Chemical Lasers

Prepared by
H. MIRELS
Aerophysics Laboratory
Laboratory Operations
The Aerospace Corporation
El Segundo, CA 90245

15 April 1986

APPROVED FOR PUBLIC RELEASE;
DISTRIBUTION UNLIMITED

Sponsored by
DEFENSE ADVANCED RESEARCH PROJECTS AGENCY
Monitored by SD under Contract No. F04701-85-C-0086

SPACE DIVISION
AIR FORCE SYSTEMS COMMAND
Los Angeles Air Force Station
P.O. Box 92960, Worldway Postal Center
Los Angeles, CA 90009-2960

DTIC
ELECTE
MAY 28 1986
E

THE VIEWS AND CONCLUSIONS CONTAINED IN THIS DOCUMENT ARE
THOSE OF THE AUTHORS AND SHOULD NOT BE INTERPRETED AS
NECESSARILY REPRESENTING THE OFFICIAL POLICIES, EITHER
EXPRESSED OR IMPLIED, OF THE DEFENSE ADVANCED RESEARCH
PROJECTS AGENCY OR THE U.S. GOVERNMENT.

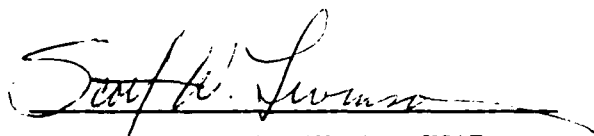
AD-A168 125

This report was submitted by The Aerospace Corporation, El Segundo, Calif. 90245, under Contract No. F04701-85-C-0086 with the Space Division, P.O. Box 92960, Worldway Postal Center, Los Angeles, Calif. 90009-2960. It was reviewed and approved for The Aerospace Corporation by W. P. Thompson, Director, Aerophysics Laboratory.

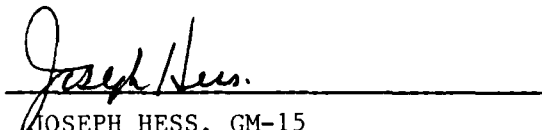
Lt Scott W. Levinson/YNS was the project officer for the Mission-Oriented Investigation and Experimentation (MOIE) Program.

This report has been reviewed by the Public Affairs Office (PAS) and is releasable to the National Technical Information Service (NTIS). At NTIS, it will be available to the general public, including foreign nationals.

This technical report has been reviewed and is approved for publication. Publication of this report does not constitute Air Force approval of the report's findings or conclusions. It is published only for the exchange and stimulation of ideas.



SCOTT W. LEVINSON, Lt, USAF
MOIE Project Officer
SD/YNS



JOSEPH HESS, GM-15
Director, AFSTC West Coast Office
AFSTC/WCO OL-AB

UNCLASSIFIED

SECURITY CLASSIFICATION OF THIS PAGE (When Data Entered)

REPORT DOCUMENTATION PAGE		READ INSTRUCTIONS BEFORE COMPLETING FORM
1. REPORT NUMBER SD-TR-86-21	2. GOVT ACCESSION NO. AD A168125	3. RECIPIENT'S CATALOG NUMBER
4. TITLE (and Subtitle) GAIN ANISOTROPY IN LOW PRESSURE CHEMICAL LASERS	5. TYPE OF REPORT & PERIOD COVERED	
7. AUTHOR(s) Harold Mirels	6. PERFORMING ORG. REPORT NUMBER TR-0086(6060)-4	
9. PERFORMING ORGANIZATION NAME AND ADDRESS The Aerospace Corporation El Segundo, Calif. 90245	8. CONTRACT OR GRANT NUMBER(s) F04701-85-C-0086	
11. CONTROLLING OFFICE NAME AND ADDRESS SDIO/DEO Office of Secretary of Defense Washington, D.C. 20301-7100	10. PROGRAM ELEMENT, PROJECT, TASK AREA & WORK UNIT NUMBERS	
14. MONITORING AGENCY NAME & ADDRESS (if different from Controlling Office) Space Division Los Angeles Air Force Station Los Angeles, Calif. 90009-2960	12. REPORT DATE 15 April 1986	
	13. NUMBER OF PAGES 16	
	15. SECURITY CLASS. (of this report) Unclassified	
	15a. DECLASSIFICATION/DOWNGRADING SCHEDULE	
16. DISTRIBUTION STATEMENT (of this Report) Approved for public release; distribution unlimited		
17. DISTRIBUTION STATEMENT (of the abstract entered in Block 20, if different from Report)		
18. SUPPLEMENTARY NOTES		
19. KEY WORDS (Continue on reverse side if necessary and identify by block number) Chemical Lasers cw Chemical Lasers Gain Anisotropy Gain Medium Diagnostics		
20. ABSTRACT (Continue on reverse side if necessary and identify by block number) The gain coefficient in a low pressure chemical laser, during lasing, differs when viewed along the optical resonator axis and when viewed normal to the axis. Expressions for axial and normal gain coefficients are deduced. The ratio of normal to axial gain coefficient is evaluated for a saturated multimode chemical laser employing a Fabry-Perot resonator. The results are useful for correlating numerical code calculations with experimental power on gain measurements made normal to the optical axis.		

DD FORM 1473
(FACSIMILE)

UNCLASSIFIED

SECURITY CLASSIFICATION OF THIS PAGE (When Data Entered)

CONTENTS

I.	INTRODUCTION.....	5
II.	THEORY.....	7
	A. Line Shape.....	7
	B. Multimode Chemical Laser.....	10
III.	CONCLUSIONS.....	19
IV.	REFERENCES.....	21

Accession For	
NTIS GRA&I	<input checked="checked" type="checkbox"/>
DTIC TAB	<input type="checkbox"/>
Unannounced	<input type="checkbox"/>
Justification	
By	
Distribution/	
Availability Codes	
Dist	Avail and/or Special
A-1	



FIGURES

1.	Coordinate System.....	8
2.	Low Pressure cw Chemical Laser with F-P Resonator.....	11
3.	Line Shape in Multimode Low Pressure cw Chemical Laser.....	13
4.	Effect of Frequency Range Parameter X_f on Gain Ratio.....	15
5.	Variation of Gain Ratio with Streamwise Distance in Saturated Multimode Low Pressure cw Chemical Laser.....	17

I. INTRODUCTION

Continuous-wave (cw) chemical lasers are frequently operated at pressures of the order of 1 Torr to achieve efficient lasing. At these pressures, the medium is inhomogeneously (Doppler) broadened, and the line shape (gain coefficient versus frequency), under power on operation, is a function of the viewing angle. For example, when viewed along the optical resonator axis, the line shape may have "holes" because of the radiation field; ^P when viewed from a direction orthogonal to the resonator axis, it is free of holes. This anisotropy of the gain medium is the subject of the present study. The purpose is to aid in the experimental validation of numerical cw chemical laser codes wherein the line shape, as viewed along the resonator axis, ^Q is predicted, and experimental measurements of power on gain are made from an orthogonal direction.

In the first portion of this study, general expressions for line shape are deduced. These expressions are then applied to determine both the axial and orthogonal gain distribution in a low pressure multimode cw chemical laser with a Fabry-Perot (F-P) resonator.

II. THEORY

A. Line shape

Consider a gain medium with mean velocity u in the x direction and thermal velocities v_x, v_y, v_z in the x, y, z directions, respectively (Fig. 1). The resonator axis is considered to be parallel to the y axis. Let ν_0 denote the resonant frequency for particles at rest. The particles with velocities v_y and v_z are resonant with frequencies¹ (i.e., Doppler effect)

$$\left(\frac{\nu}{\nu_0} - 1 \right)_y = \frac{v_y}{c} \quad (1a)$$

$$\left(\frac{\nu}{\nu_0} - 1 \right)_z = \frac{v_z}{c} \quad (1b)$$

for radiation in the y and z directions, respectively. Particle velocity and resonant frequency can be used interchangeably. Consider a two-level model and introduce the notation

$$\Delta n \equiv n_2 - n_1 \quad (2a)$$

$$[\Delta n(\nu)]_y \equiv [n_2(\nu) - n_1(\nu)]_y \quad (2b)$$

$$[\Delta n(\nu)]_z \equiv [n_2(\nu) - n_1(\nu)]_z \quad (2c)$$

where Δn is the net difference between the number of particles, per unit volume, in the upper (subscript 2) and lower (subscript 1) lasing levels. The quantities $[\Delta n(\nu)]_y d\nu$ and $[\Delta n(\nu)]_z d\nu$ denote the number of particles in the frequency interval ν to $\nu + d\nu$ that are resonant with radiation in the y and z directions, respectively. The Doppler broadened gain coefficient in the y and z directions is then

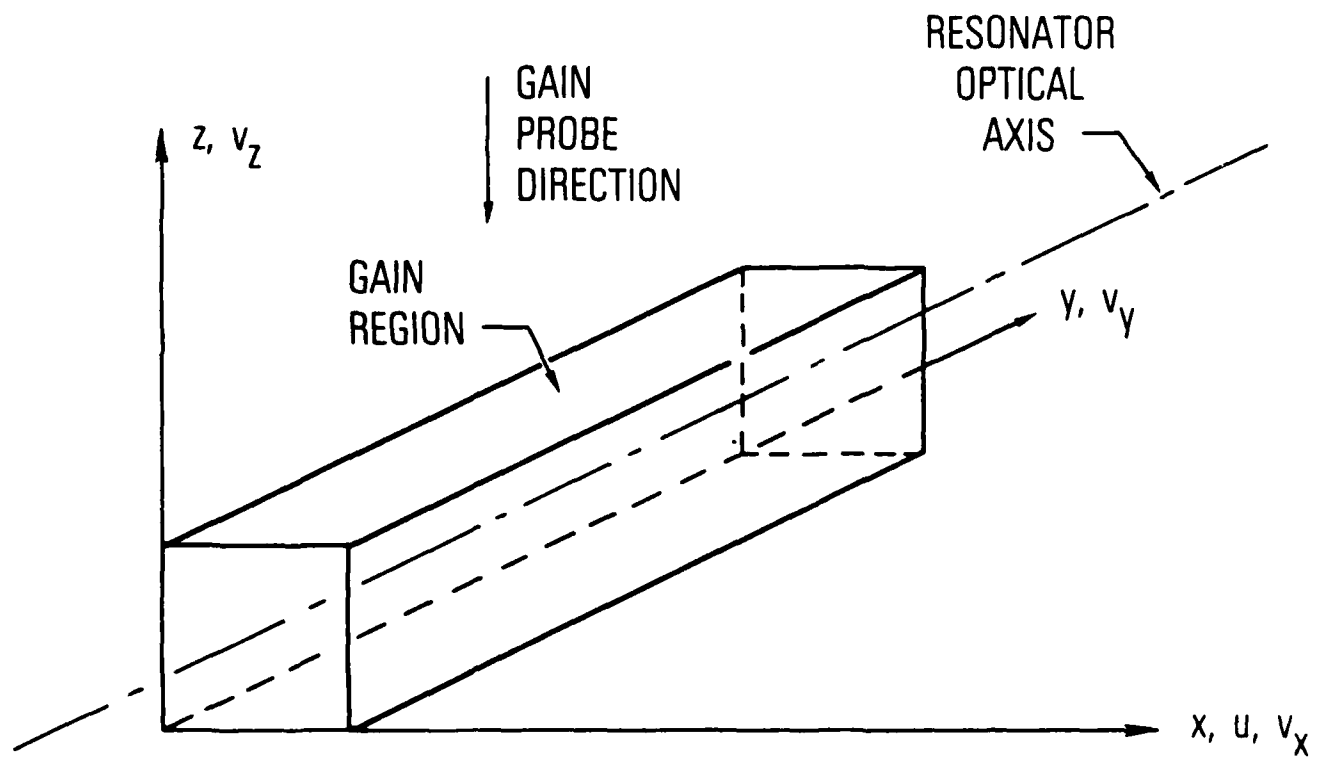


Fig. 1. Coordinate system.

$$g_y(v) = \sigma_0 \int_{-\infty}^{\infty} L(v-v') [\Delta n(v')]_y dv' \quad (3a)$$

$$g_z(v) = \sigma_0 \int_{-\infty}^{\infty} L(v-v') [\Delta n(v')]_z dv' \quad (3b)$$

where

$$L(v-v') = \frac{\sigma(v, v')}{\sigma_0} = \left[1 + 4 \left(\frac{v-v'}{\Delta v_h} \right)^2 \right]^{-1} \quad (3c)$$

Here Δv_h is the homogeneous width (FWHM) for the medium, $\sigma(v, v')$ is the cross section for stimulated emission at v resulting from particles with "velocity" v' and σ_0 denotes $\sigma(v_0, v_0)$.

The quantity $[\Delta n(v')]_y$, in Eq. (3a) is found from a consideration of the optical resonator and may exhibit holes in the vicinity of optical mode frequencies.³ However, $[\Delta n(v')]_z$ has a Maxwellian distribution because there are no external factors that disturb the equilibrium in the z direction. Thus

$$\frac{[\Delta n(v)]_z}{\Delta n} = \bar{p}_0 \exp(-X^2) \quad (4a)$$

where

$$\bar{p}_0 \equiv [(4 \ln 2)/\pi]^{1/2} / \Delta v_d \quad (4b)$$

$$X \equiv (4 \ln 2)^{1/2} (v-v_0) / \Delta v_d \quad (4c)$$

and Δv_d is the Doppler width (FWHM).*

* $\Delta v_d / v_0 = [8(\ln 2)kT/m]^{1/2} / c.$

We now consider the limit $\Delta v_h / \Delta v_d \rightarrow 0$. The quantity $\Delta n(v')$ can be evaluated at $v' = v$ in Eqs. (3a), and (3b); these become

$$g_y(v) = (\pi/2) \sigma_o \Delta v_h [\Delta n(v)]_y \quad (5a)$$

$$g_z(v) = (\pi/2) \sigma_o \Delta v_p \bar{p}_o \Delta n \exp(-X^2) \quad (5b)$$

Also,

$$\frac{g_y(v)}{g_z(v)} = \frac{[\Delta n(v)]_y}{\bar{p}_o \Delta n \exp(-X^2)} \quad (6)$$

Thus, in the present limit, the ratio of the gain at frequency v in the y and z direction is simply equal to the ratio of the number density of the particles that are resonant with the radiation in y and z directions, respectively. Numerical estimates for $g_y(v)/g_z(v)$, for a multimode chemical laser, are obtained in the next section using the results of References 3 and 4.

B. Multimode Chemical Laser

We consider a multimode low pressure cw chemical laser in the limit $\Delta v_h / \Delta v_d \rightarrow 0$. An F-P resonator is assumed. The laser is illustrated in Fig. 2. It is assumed that the F-P resonator is in perfect alignment and that no diffractive coupling occurs between the optical modes at adjacent streamwise stations. It is assumed further that the mirror separation L is sufficiently large that the longitudinal mode separation $\Delta v_c = c/(2L)$ is of order Δv_h or smaller. The latter assumption results in a large number of longitudinal

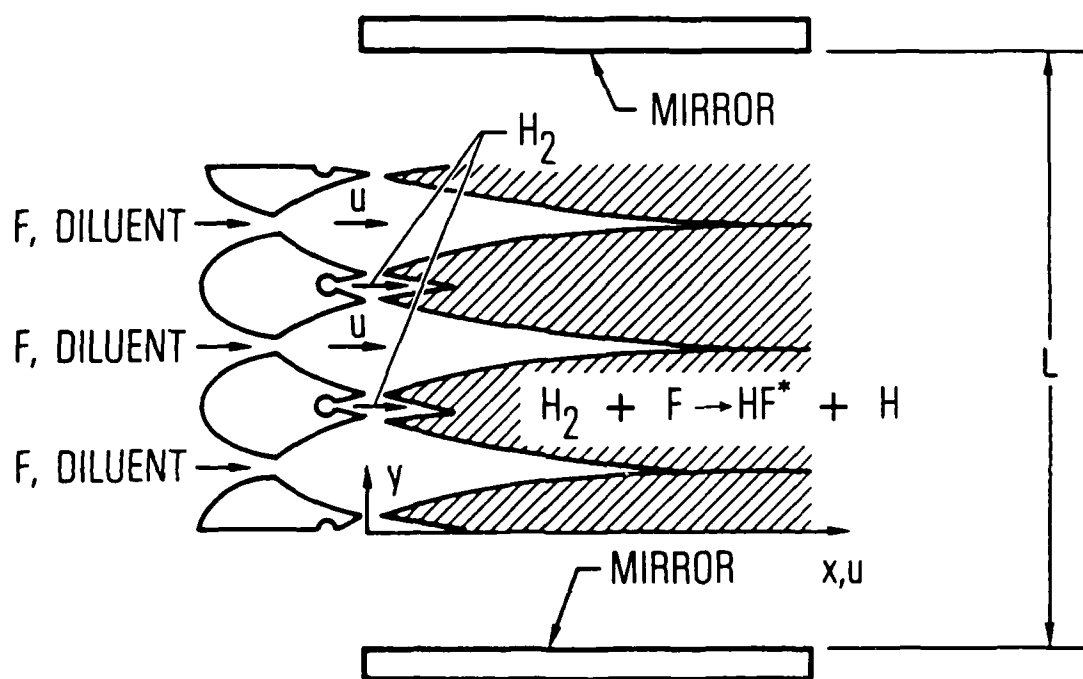


Fig. 2. Low pressure cw chemical laser with F-P resonator.

modes that truncate the line shape, when viewed along the optical axis, as indicated in Fig. 3. The performance of this laser was evaluated in Reference 3 using a two-level model. The corresponding gain, when viewed in the z direction, is obtained here.

Let $\zeta = k_{cd} x/u$ be a normalized streamwise distance, where k_{cd} is a characteristic deactivation rate, and let ν_f denote the highest longitudinal mode frequency which is excited at each streamwise station. Introduce

$$X_f = (4 \ln 2)^{1/2} (\nu_f - \nu_o) / \Delta \nu_d \quad (7)$$

which is a function of ζ . The number of longitudinal modes, at each streamwise station, equals $(\nu_f - \nu_o) / \Delta \nu_c$ and is large because $\Delta \nu_c$ is small. The resultant line shape, when viewed from the y and z directions, is illustrated in Fig. 3. The variation of $[\Delta n(\nu)]_z / (\bar{p}_o \Delta n)$ with frequency is Maxwellian as indicated in Eq. (5b). The variation of $[\Delta n(\nu)]_y / (\bar{p}_o \Delta n)$ with frequency is flat, in the range $|X| < X_f$ because lasing suppresses the gain coefficient to the resonator threshold value, g_c . However, the variation of $[\Delta n(\nu)]_y / (\bar{p}_o \Delta n)$ with frequency is Maxwellian in the range $|X| > X_f$. The condition that the net number density difference Δn be the same, when viewed from either the y or z directions, indicates that the area under each of the curves, in Fig. 3, is the same. Hence these curves are related by the expressions*

*Note from Fig. 3 that there are more upper level particles with large thermal velocities in the $\pm y$ direction than there are upper level particles with large thermal velocities in the $\pm z$ direction. This is because upper level particles with velocities v_y that correspond to $|X| > X_f$ are unaffected by the radiation field whereas upper level particles with velocity v_z are "homogeneously" deactivated by the radiation field.

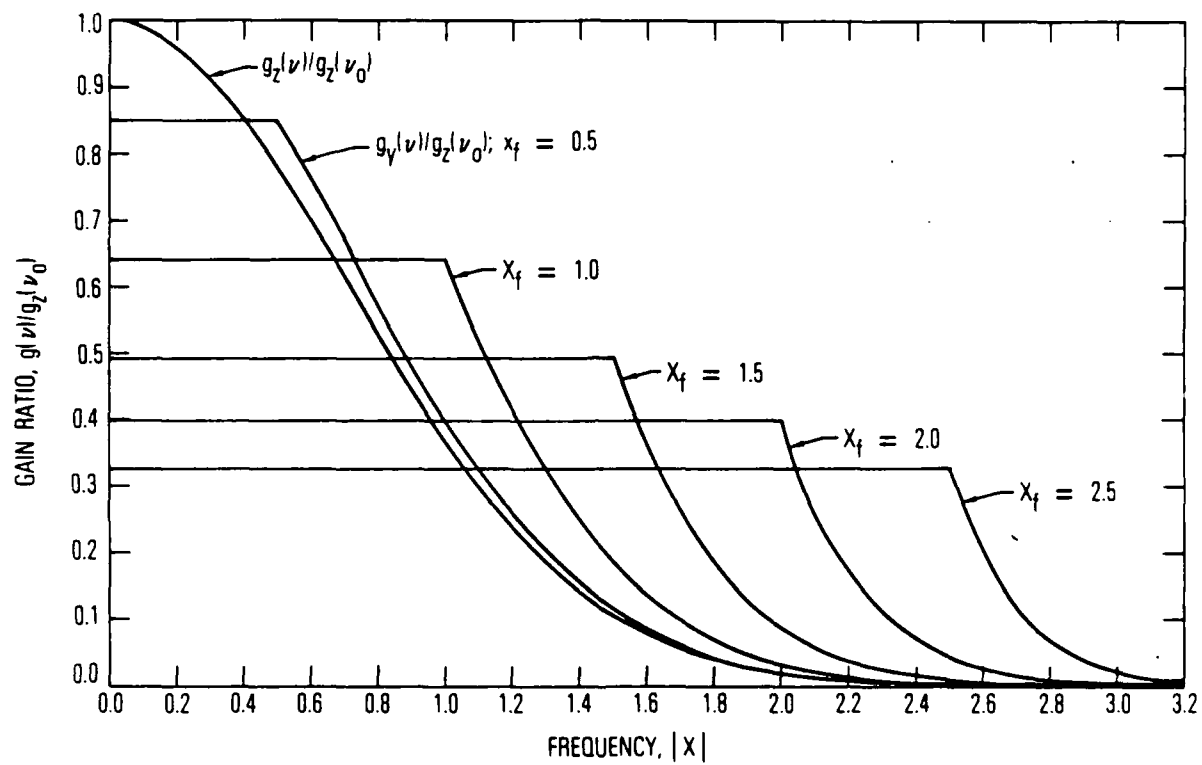


Fig. 3. Line shape in multimode low pressure cw chemical laser.

$$\frac{[\Delta n(v)]_z}{\bar{p}_0 \Delta n} = \exp(-X^2) \quad (8a)$$

$$\frac{[\Delta n(v)]_y}{\bar{p}_0 \Delta n} = \left[\frac{2X_f}{\pi^{1/2}} + \exp(X_f^2) \operatorname{erfc} X_f \right]^{-1} \quad |X| < X_f \quad (8b)$$

$$= []^{-1} \exp(X_f^2 - X^2) \quad |X| > X_f \quad (8c)$$

The gain ratio, at v_0 , is simply

$$\frac{g_z(v_0)}{g_y(v_0)} = \frac{2X_f}{\pi^{1/2}} + \exp(X_f^2) \operatorname{erfc} X_f \quad (9)$$

which is plotted in Fig. 4. The ratio is a function of X_f , which, as previously noted, is a measure of the number of longitudinal modes excited at each streamwise station ζ .

An analytic solution can be obtained for the variation of g_z/g_y with streamwise distance by considering the limit

$$R \equiv \frac{k_{cr}}{k_{cd}} \gg 1; \quad \frac{g_c}{g_{mzp}} \ll 1; \quad R \frac{g_c}{g_{mzp}} = 0(1) \quad (10)$$

Here R is the ratio of the translational cross relaxation rate to the collisional deactivation rate and has a value of order 100.³ The quantity g_c/g_{mzp} is the ratio of resonator threshold gain g_c to the maximum zero power gain that is achieved in the laser medium, g_{mzp} . The latter is the line center gain at $\zeta = 0.3051$ under nonlasing conditions.³ The ratio g_c/g_{mzp} typically equals 0.01 in a highly saturated laser. Hence the assumption $Rg_c/g_{mzp} = 0(1)$ is realistic. The variation of X_f with ζ is then⁴ (for $\zeta \neq 0$)

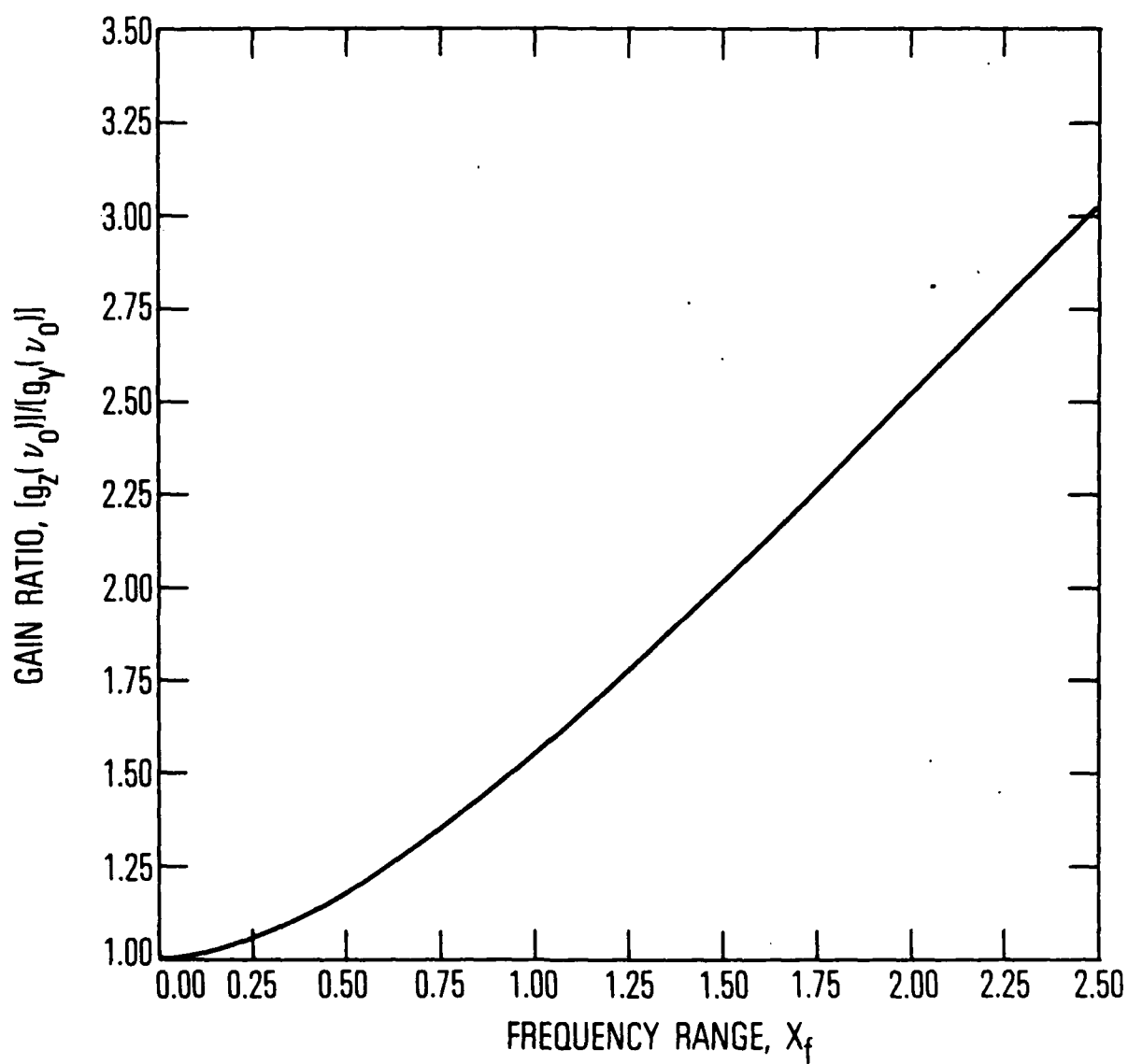


Fig. 4. Effect of frequency range parameter X_f on gain ratio.

$$\zeta = [(2 + \beta^2)^{1/2} - \beta]^2 / 4 \quad (11a)$$

$$\beta = \frac{2}{\pi} \left(\frac{R}{1.804} \frac{g_c}{g_{mzp}} \right) \left[\exp(X_f^2) \operatorname{erf} X_f - \frac{2 X_f}{\pi^{1/2}} \right] \quad (11b)$$

The variation of $g_y(v_o)/g_z(v_o)$ with streamwise distance is obtained from Eqs. (9) and (11) and is plotted in Fig. 5 as a function of laser saturation level. The lasing region extends from $\zeta = 0$ to $\zeta = 1/2$. The ratio $g_z(v_o)/g_y(v_o)$ varies from values of 1.5 to 2.5 near $\zeta = 0$ to the value 1, at $\zeta = 1/2$. The gain ratio increases as the degree of saturation increases (i.e., as Rg_c/g_{mzp} decreases). For an F-P resonator, $g_y(v_o) = g_c$, so that the ordinate in Fig. 5 can be interpreted as $g_z(v_o)/g_c$. The corresponding values of X_f vary from 1.0 to 2.0 near $\zeta = 0$ to 0 near $\zeta = 1/2$ as may be inferred from Figs. 4 and 5. The present results require perfect alignment of the F-P resonator and no diffractive coupling between adjacent streamwise stations, as was previously assumed.

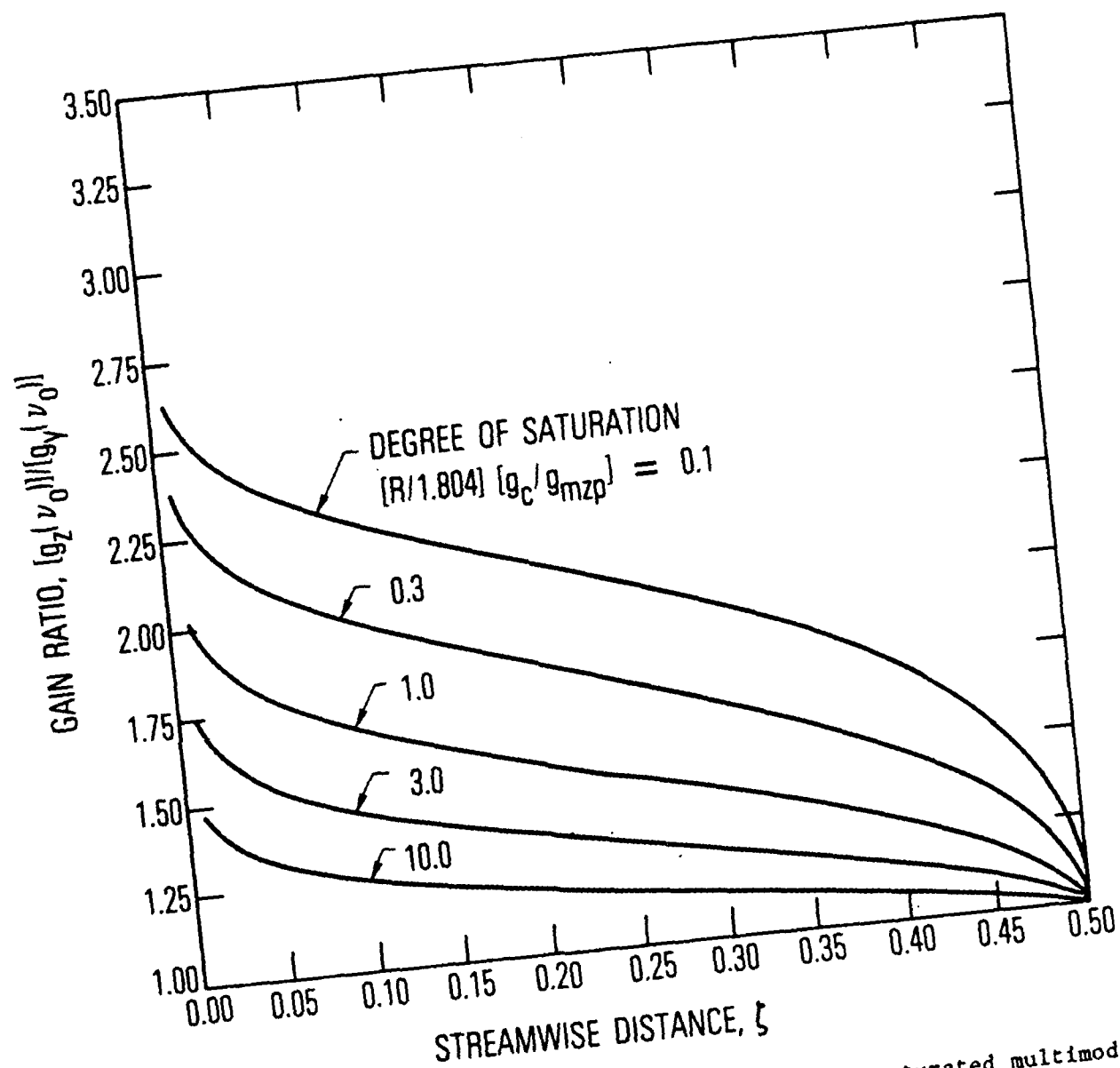


Fig. 5. Variation of gain ratio with streamwise distance in saturated multimode low pressure cw chemical laser.

III. CONCLUSIONS

The present study has discussed gain anisotropy in low pressure cw chemical lasers and has provided numerical results for the case of a saturated multimode laser with an F-P resonator. Values of the gain ratio $g_z(v_o)/g_y(v_o)$ up to about 2.5 were obtained for the particular cases considered herein. It may be concluded that the gain ratio differs significantly from one during leasing.

The value of $g_z(v_o)/g_y(v_o)$ can be easily obtained in the course of numerical resonator calculations for low pressure chemical lasers. Such codes (e.g., Reference 2) presently compute $g_y(v_o)$ and the local net inversion. The corresponding value of $g_z(v_o)$ is obtained from the local net inversion by assuming a Maxwellian velocity distribution [e.g., Eq. (5b)]. Hence, experimental power on measurements of $g_z(v_o)$ can be used to provide a check of numerical code predictions.

The effect of source flow on gain anisotropy can be deduced from Ref. 5 and has not been considered herein.

IV. REFERENCES

1. M. Sargent II, M. O. Scully, and W. E. Lamb, Jr., Laser Physics (Addison-Wesley, Reading, Mass., 1974) pp. 144-155.
2. D. L. Bullock, M. M. Valley, and R. S. Lipkis, "Advanced Chemical Laser Optics Study," TRW Final Report, Contract No. F29601-79-C-0022, CDRL Item A005, 15 July 1982.
3. H. Mirels, AIAA J. 17, 478 (1979).
4. H. Mirels, Appl. Opt. 20, 362 (1981).
5. H. Mirels, Appl. Opt. 20, 835 (1981).

LABORATORY OPERATIONS

The Aerospace Corporation functions as an "architect-engineer" for national security projects, specializing in advanced military space systems. Providing research support, the corporation's Laboratory Operations conducts experimental and theoretical investigations that focus on the application of scientific and technical advances to such systems. Vital to the success of these investigations is the technical staff's wide-ranging expertise and its ability to stay current with new developments. This expertise is enhanced by a research program aimed at dealing with the many problems associated with rapidly evolving space systems. Contributing their capabilities to the research effort are these individual laboratories:

Aerophysics Laboratory: Launch vehicle and reentry fluid mechanics, heat transfer and flight dynamics; chemical and electric propulsion, propellant chemistry, chemical dynamics, environmental chemistry, trace detection; spacecraft structural mechanics, contamination, thermal and structural control; high temperature thermomechanics, gas kinetics and radiation; cw and pulsed chemical and excimer laser development including chemical kinetics, spectroscopy, optical resonators, beam control, atmospheric propagation, laser effects and countermeasures.

Chemistry and Physics Laboratory: Atmospheric chemical reactions, atmospheric optics, light scattering, state-specific chemical reactions and radiative signatures of missile plumes, sensor out-of-field-of-view rejection, applied laser spectroscopy, laser chemistry, laser optoelectronics, solar cell physics, battery electrochemistry, space vacuum and radiation effects on materials, lubrication and surface phenomena, thermionic emission, photo-sensitive materials and detectors, atomic frequency standards, and environmental chemistry.

Computer Science Laboratory: Program verification, program translation, performance-sensitive system design, distributed architectures for spaceborne computers, fault-tolerant computer systems, artificial intelligence, micro-electronics applications, communication protocols, and computer security.

Electronics Research Laboratory: Microelectronics, solid-state device physics, compound semiconductors, radiation hardening; electro-optics, quantum electronics, solid-state lasers, optical propagation and communications; microwave semiconductor devices, microwave/millimeter wave measurements, diagnostics and radiometry, microwave/millimeter wave thermionic devices; atomic time and frequency standards; antennas, rf systems, electromagnetic propagation phenomena, space communication systems.

Materials Sciences Laboratory: Development of new materials: metals, alloys, ceramics, polymers and their composites, and new forms of carbon; non-destructive evaluation, component failure analysis and reliability; fracture mechanics and stress corrosion; analysis and evaluation of materials at cryogenic and elevated temperatures as well as in space and enemy-induced environments.

Space Sciences Laboratory: Magnetospheric, auroral and cosmic ray physics, wave-particle interactions, magnetospheric plasma waves; atmospheric and ionospheric physics, density and composition of the upper atmosphere, remote sensing using atmospheric radiation; solar physics, infrared astronomy, infrared signature analysis; effects of solar activity, magnetic storms and nuclear explosions on the earth's atmosphere, ionosphere and magnetosphere; effects of electromagnetic and particulate radiations on space systems; space instrumentation.

...

END
DITIC

7-86